



ELSEVIER

Available online at [www.sciencedirect.com](http://www.sciencedirect.com)

SCIENCE @ DIRECT®

Journal of Chromatography A, 1018 (2003) 183–196

JOURNAL OF  
CHROMATOGRAPHY A

[www.elsevier.com/locate/chroma](http://www.elsevier.com/locate/chroma)

## Enhanced calculation of optimal gradient programs in reversed-phase liquid chromatography<sup>☆</sup>

G. Vivó-Truyols, J.R. Torres-Lapasió\*, M.C. García-Alvarez-Coque

*Departamento de Química Analítica, Universitat de València, c/Dr. Moliner 50, 46100 Burjassot, Spain*

Received 14 April 2003; received in revised form 21 July 2003; accepted 18 August 2003

### Abstract

The resolution of a mixture of 16  $\beta$ -blockers under gradient elution was optimised using both isocratic and gradient training sets, with a reversed-phase column and acetonitrile–water eluents. Error theory was applied to measure the information extracted from different gradient experimental designs. This allows checking the expected accuracy when gradient predictions exceed the initial solvent concentrations tested in the training set. This work applies the results on modelling found in a previous study [J. Chromatogr. A 1018 (2003) 169] where the performance of several retention models was compared. Enhanced retention predictions were applied to the optimisation of gradient programs involving three factors (gradient slope, initial solvent composition and gradient curvature), using the peak purity criterion as resolution assessment. Peak shape parameters required in peak purity evaluation were modelled by adapting previous developments in isocratic mode. The mixture, which required prohibitive analysis times under isocratic elution, was almost baseline resolved in less than 35 min with linear gradients. Curvilinear gradients did not enhance this result significantly.

© 2003 Elsevier B.V. All rights reserved.

**Keywords:** Gradient elution; Optimisation; Error analysis; Resolution; Peak purity;  $\beta$ -Blockers

### 1. Introduction

High performance liquid chromatography (HPLC) has become a primary analytical technique forming the basis of many reference procedures. For routine analysis, isocratic elution is a preferred separation mode. Some reasons that may justify this prevalence are the lower cost, simpler instrumentation, and no

need of column re-equilibration between consecutive injections. The practical utility of isocratic HPLC is, however, limited to sets of compounds exhibiting a relatively narrow range of polarities. Some compounds are scarcely retained whilst others elute under unpractically long analysis times. A common solution to overcome such situations consists of increasing progressively the elution strength of the mobile phase as the analysis progresses (i.e. gradient elution), which expedites the elution of the most retained compounds. This can be carried out in many ways, which is translated in a virtually unlimited number of gradient programs, most of which will not resolve the mixture.

<sup>☆</sup> This work was presented at the 24th International Symposium on Chromatography, Leipzig (Germany), September 2002.

\* Corresponding author. Tel.: +34-963543003; fax: +34-963544436.

E-mail address: [jrtorres@uv.es](mailto:jrtorres@uv.es) (J.R. Torres-Lapasió).

Trial-and-error optimisations are frequently used to find out appropriate gradients, although they are particularly slow and inefficient. These limitations may explain the effort that has been invested in computer-assisted strategies. Some software packages including gradient optimisation facilities, such as Dry-Lab [1,2], Preopt-W [3], Osiris [4] and ChromSword [5], are currently available. However, although gradient optimisation has reached a routine level, some topics still remain controversial.

The main factor to be enhanced in order to obtain realistic optimisations is the achievement of predictions of retention as accurate as possible. This requires to consider the elution mode (i.e. isocratic or gradient), the data gathered come from, since the quality of the achieved information will depend on the origin of the data used to model the retention. Also, this information should be contrasted with that required in the optimisation process. Several studies about how to plan gradient designs to predict the retention have been published [6,7]. Some recommendations have arisen about the adequate gradient slopes to model the system for gradient [8] and isocratic [9] predictions. A previous work applies the error propagation theory to the analysis of the amount of information about retention contained in isocratic and gradient experimental designs [10]. This approach is proposed in this work to prospect whether predictions of retention deteriorate significantly by increasing the initial solvent concentration of the gradient program. This change may imply an extrapolation of the retention for certain solutes.

Besides the experimental design, a fundamental topic affecting the quality of predictions is the equation selected to fit the training data. Linear and parabolic models relating the logarithm of the retention factor and the concentration of organic modifier are common models to describe retention in RPLC [11], although other equations based on linear solvation approaches have been proposed and tested successfully for isocratic [12,13] and gradient [10] predictions.

Once the retention has been appropriately modelled, a further step consists of optimising the gradient program. Gradient optimisation can be performed in several ways, depending on the selected factors that parameterise the gradient profile. Jandera [14] proposed the optimisation of gradient time, gradient

shape and initial composition of the mobile phase. Snyder et al. [15] and Chaminade et al. [16] optimised simple- and multi-linear gradients. Cela and Lores [3] approximated the gradients to a limited number of isocratic steps.

Another point that should be considered in any optimisation is the chromatographic objective function (COF) that should quantify the resolution of each peak or peak pair. A COF with a particularly good performance that has been used in isocratic optimisation is the peak purity or free-area fraction [17,18]. This measurement allows a realistic evaluation of the separation degree achieved in a given chromatogram, and will be used in this work for gradient optimisation. For this purpose, efficiency and peak asymmetry were modelled for each peak as a function of mobile phase composition, and applied to predict peak shape in gradient elution.

The optimisation of the separation of a mixture of 16  $\beta$ -blockers using gradient elution was studied. This elution mode was needed to resolve the compounds with a reasonable analysis time.  $\beta$ -Blockers are clinically important drugs used in the treatment of neurological, neuropsychiatric and cardiovascular disorders [19]. They are also abused in sports due to their blood pressure regulatory and tremor decreasing effects. The retention behaviour of each  $\beta$ -blocker was modelled from isocratic and gradient experiments, using a reversed-phase column and acetonitrile in the mobile phase. The performance of several models that describe the retention was checked. Error theory was used to examine the information extracted from gradient experimental designs to predict different gradients out of the initial domain. The benefits achieved from this study were applied to optimise a gradient separation involving three factors (gradient slope, initial solvent composition and curvature), using the peak purity criterion as resolution assessment.

## 2. Theory

In gradient elution, the goal of interpretive optimisations is to establish, from a set of experiments as reduced as possible, the profile in solvent increment that will yield a chromatogram with an optimal separation. This is a numerical problem, usually solved by exploring the performance of hundreds of gradient profiles.

Each gradient profile is characterised by one or more descriptors that are regularly varied throughout the optimisation process to find the best conditions. For each tentative gradient program, the overall resolution of the corresponding computer-generated chromatogram is evaluated. That chromatogram having the maximal COF value will denote the best gradient profile. Computer predictions are taking benefit of the advances in modelling of gradient retention times, peak widths and asymmetries, which are incorporated in a peak model to obtain realistic simulations of chromatograms. In summary, the resolution task involves the calculation of gradient retention times, peak widths and asymmetries for each solute under each candidate gradient program.

### 2.1. Modelling of retention

The first step in the optimisation of the resolution of a mixture is gathering, for each compound, information about its retention behaviour. This will allow to infer a relationship to predict the retention time as a function of solvent concentration. The retention model can be fitted from either isocratic or gradient experiments, which means finding the best values of the model parameters for each solute under a least-squares basis. For this purpose, a convenient algebraic expression or black-box algorithm, able to predict the isocratic or gradient retention times as a function of solvent content or gradient program, should be available. However, the performance of the equations used to model the retention also depends strongly on other factors, such as experimental design, elution mode and solvent range where the retention was measured. Also, the elution mode where the predictions should be done may influence the performance of the equations [10]. In gradient predictions, the gradient profile being checked is another important factor. The suitable equations to predict the gradient retention were studied elsewhere [10] and will not be detailed here.

Three equations were considered to describe the retention behaviour:

$$\log k = c_0 + c_1\varphi \quad (1)$$

$$\log k = c_0 + c_1\varphi + c_2\varphi^2 \quad (2)$$

$$\log k = c_0 + c_1 P_m^N = c_0 + c_1 \left( 1 - \frac{1.33\varphi}{1 + 0.47\varphi} \right) \quad (3)$$

where  $k$  is the retention factor,  $\varphi$  the volume fraction of organic solvent in the mobile phase, and  $c_0$ ,  $c_1$  and  $c_2$  model parameters;  $P_m^N$  is a modified polarity parameter [12,13].

These three models (Eqs. (1)–(3)) can be used to predict gradient retention times ( $t_g$ ), by resolving the integral equation given by Eq. (5) in [10]. When linear gradients are being considered and Eq. (1) is the selected retention model (linear solvent strength theory [20,21]), this integral equation has an algebraic solution (Eq. (11) in [10]). In other cases (i.e. other gradient profiles, or when Eqs. (2) and (3) are used as retention models), the integral lacks of an algebraic solution, and the gradient retention time should be obtained through numerical integration. In this work, a previously reported method [10] was applied.

When Eqs. (1)–(3) were fitted from isocratic data, the model parameters were straightforwardly obtained through multiple linear regression. Otherwise, since non-linear equations were involved, the Powell method [22] was chosen to fit the data.

### 2.2. Prediction of peak shape

The usual definition of chromatographic efficiency ( $N$ ), which assumes a straightforward relationship between  $\sqrt{N}$  and the retention time-to-peak width ratio ( $t_R/W$ ), does not hold in gradients. As a consequence, extended definitions of efficiency for asymmetrical peaks as the following [23]:

$$N = \frac{41.7(t_R/W)^2}{(B/A) + 1.25} \quad (4)$$

are similarly unsuited. In Eq. (4),  $W$  and  $B/A$  are peak width and asymmetry factor, respectively, measured at 10% of peak height.

In a first approximation, both the efficiency and the asymmetry factor can be considered constant for all solutes and independent of  $\varphi$ . However, more accurate predictions may be carried out by taking into account their variations with solvent composition, which in addition are different for each solute. In isocratic optimisation, local linear models on  $\varphi$  have been successfully used to predict  $N$  and  $B/A$  for each solute [24]. This approach was here adapted to gradient elution. For this purpose, the bandwidth of a given solute was predicted according to Jandera [25], by approximating it to the bandwidth that would be obtained

if the solute eluted isocratically at the mobile phase composition measured at the column outlet when the solute leaves the column under gradient elution. Peak asymmetry was computed in a similar way. If gradient values of  $W$  and  $B/A$  are assumed to be related to the corresponding isocratic values, application of Eq. (4) is possible in the gradient case. Gradient predictions can be thus benefited of the developments on peak shape modelling in isocratic conditions.

Prediction of peak shape was thus performed in two steps. In a first step, models of  $N$  and  $B/A$  were built as a function of modifier concentration. For isocratic-to-gradient predictions, the fittings were straightforward. In the gradient-to-gradient case, the solvent concentration affecting the solute when it leaves the column was estimated for each training gradient, which allowed the calculation of  $N$  and  $B/A$  for the corresponding isocratic compositions. Then, local linear models were established with these values as a function of modifier content, which made the predictions similar to the isocratic-to-gradient case.

In a second step, the isocratic models for  $N$  and  $B/A$  were used to predict gradient peak shapes. Thus, the concentration of  $\varphi$  at which the solute leaves the column was first calculated for a given gradient, and the corresponding  $N$  and  $B/A$  values were interpolated for each solute in the established isocratic models. The retention time of the solute eluted isocratically under this solvent concentration was also calculated. These values were used to depict the peak profiles in the simulated chromatogram.

### 2.3. Simulated chromatograms and resolution maps

Once succeeded in the prediction of the retention time, efficiency and asymmetry for all solutes for any gradient program, the corresponding theoretical chromatogram can be simulated. Since the procedure can be found elsewhere [26], only some details will be given here. As peak model, a modified Gaussian with a standard deviation varying linearly with the distance to the peak maximum was used [24], but other models are also available in the literature [27]. The advantage of the selected model, besides its simplicity, is the facility in relating its four parameters to convenient peak properties (efficiency, asymmetry factor, peak height—or area—and retention time).

Several resolution descriptors can be applied to quantify the separation of each peak or peak pair. One of them is the peak purity,  $p$ , whose meaning is extremely intuitive, easy and interpretable: it depicts the area percentage free of interference of the peak of a given solute [28]. Peak purity is an intrinsically normalised assessment, related to each peak (not to each peak pair). Comparisons between  $p$  and other measurements such as  $R_S$  can be found elsewhere [17,26,29]. Applications of peak purity in conventional and especial optimisations can be found for instance in [30,31].

Chromatographic optimisation requires a reduction of the information contained in a simulated chromatogram to a single value depicting the resolution of all the peaks as a whole. If a chromatogram involves  $ns$  solutes, the reduction can be done, for instance, by calculating the overall peak purity, which is given by [17]

$$P = \prod_{s=1}^{ns} p_s = \prod_{s=1}^{ns} \left( 1 - \frac{w'_s}{w_s} \right) \quad (5)$$

where  $w_s$  is the total peak area of solute  $s$ , whose peak purity is  $p_s$ , and  $w'_s$ , the area of this peak that is overlapped by the chromatogram originated by the remaining compounds.

The resolution map is built by computing the  $P$ -values, for a regular distribution of gradient program descriptors. Three descriptors were considered in this work: the gradient time ( $t_G$ ), the concentration of organic solvent at the beginning of the gradient ( $\varphi_0$ ), and the gradient curvature ( $n$ ). Given a ( $t_G$ ,  $\varphi_0$ ,  $n$ ) set, the associated gradient program  $\varphi(t)$  was defined as follows [20]:

$$\varphi(t) = \begin{cases} \varphi_0, & \text{if } t < t_D \\ \varphi_0 + (\varphi_f - \varphi_0) \left[ 1 - \left( 1 - \frac{t - t_D}{t_G} \right)^{1/n} \right], & \text{if } t \geq t_D \text{ and } n < 1 \\ \varphi_0 + (\varphi_f - \varphi_0) \left( \frac{t - t_D}{t_G} \right)^n, & \text{if } t \geq t_D \text{ and } n \geq 1 \end{cases} \quad (6)$$

where  $\varphi_0$  and  $\varphi_f$  are the solvent concentration at the beginning and the end of the gradient, respectively,  $t_D$  the time delay till the gradient front reaches the

column inlet (dwell time) and  $t_G$  the time required for the gradient scan (gradient time). Values of  $n$  smaller and larger than 1 yield convex and concave gradients, respectively. Finally, gradients with  $n = 1$  are linear.

#### 2.4. Information about retention contained in a given gradient design

A method based on the error propagation theory is introduced in this section to assess the information associated to gradient designs. This approach can help the chromatographer to foresee how informative are the collected data in order to make gradient predictions. A straightforward application of this capability is the estimation of the extrapolation degree that new gradient conditions would demand, taking into account the information provided by the experimental data. An example can be found in predictions where the fitting is carried out with gradients starting at a solvent concentration larger than the values used in the modelling step (see Section 4.2.4). The selection of the retention model should consider these extrapolation requirements.

Retention time prediction in gradient mode from gradient experimental data is a two-step process. The first step consists of establishing an isocratic retention model using the collected gradient data, whereas in the second one the fitted model is used to predict the wished gradient. Thus, there is an implicit modelling of the retention behaviour depending on only one subjacent factor (i.e. the concentration of organic solvent), although the descriptors associated to a gradient are at least two (i.e.  $t_G$  and  $\varphi_0$ ). Therefore, a study concerning the variation of these two descriptors may be redundant. The evaluation of the quality of the information is easier if it is expressed as a function of the factor actually fitted ( $\varphi$ ), instead of the two variables defining the gradient.

The procedure followed to compute the amount of information is next described:

- (i) The retention model is first fitted using data acquired according to a given gradient experimental design. In the example given, four gradient runs were carried out by varying the composition from 5 to 30% acetonitrile in  $t_G = 20, 30, 40$  and 50 min.

- (ii) The Jacobian matrix,  $\mathbf{J}_{\text{grd}}$ , associated to this experimental design is calculated. The  $j_{\text{grd}}(i,j)$  element of this matrix is defined as

$$j_{\text{grd}}(i, j) = \frac{\partial \hat{t}_{g,i}}{\partial b_j} \quad (7)$$

where  $\hat{t}_{g,i}$  is the calculated gradient retention time for the  $i$ th gradient program of the experimental design, and  $b_j$  the  $j$ th parameter of the retention model. Note that  $\mathbf{J}_{\text{grd}}$  depends on the retention model.

- (iii) The Jacobian matrix for the isocratic retention,  $\mathbf{J}_{\text{iso}}$ , is calculated for a regular distribution of mobile phases. Analogously to Eq. (7), the  $j_{\text{iso}}(i,j)$  element of this matrix is defined as the derivative of  $\hat{t}_{\text{R}}$  calculated for the  $i$ th isocratic experiment with respect to the  $j$ th parameter of the retention model.
- (iv) The amount of information,  $\epsilon$ , is given by

$$\epsilon = \frac{\hat{t}_{\text{R}}^2}{\mathbf{J}_{\text{iso}}(\mathbf{J}_{\text{grd}}^T \mathbf{J}_{\text{grd}})^{-1} \mathbf{J}_{\text{iso}}^T} \quad (8)$$

where  $\hat{t}_{\text{R}} = (\hat{t}_{\text{R},1}, \hat{t}_{\text{R},2}, \dots, \hat{t}_{\text{R},m})$  contains the calculated retention times for the mobile phases denoted by the subindex, and  $\epsilon = (\epsilon_1, \epsilon_2, \dots, \epsilon_m)$  is a vector whose elements store the amount of information associated to each mobile phase. Note that the denominator of Eq. (8) is the definition of the variance in the isocratic prediction, although it lacks of the pure experimental error term. In this case, the computation of the pure error is not required, since the amount of information is used only as a relative parameter.

- (v) In the four studied gradients, each solute left the column before the final acetonitrile concentration (30% acetonitrile) was reached. These critical compositions are specific for each gradient and solute. Above these values, gradients are unable to provide information about retention. The faster the gradient (i.e. the smaller the  $t_G$ ), the larger this concentration. For each solute, the maximal critical concentration found in the studied gradients was taken to trim the  $\epsilon$ -values: those corresponding to acetonitrile concentrations above this limiting value were set to zero.

- (vi) The normalised amount of information,  $\epsilon_{\text{norm}}$ , is finally obtained. This parameter, which is calculated by dividing  $\epsilon$  by its Euclidean norm:

$$\epsilon_{\text{norm}} = \frac{\epsilon}{\|\epsilon\|} \quad (9)$$

allows easier comparisons for different solutes and experimental designs than  $\epsilon$ .

### 3. Experimental

Sixteen  $\beta$ -blockers were studied: acebutolol, alprenolol, atenolol, bisoprolol, carteolol, celiprolol, esmolol, labetalol, metoprolol, nadolol, oxprenolol, pindolol, practolol, propranolol, sotalol, and timolol. The drugs were dissolved in a small amount of methanol and diluted with water. The concentration of the injected solutions was 10  $\mu\text{g/ml}$ . Mobile phases were prepared with acetonitrile (Scharlab, Barcelona, Spain), and buffered at pH 3 with di-sodium hydrogen phosphate and hydrochloric acid (Panreac, Barcelona). The concentration of organic solvent is given as volumetric fraction percentage.

An Agilent chromatograph (Model HP 1100, Palo Alto, CA, USA), equipped with a quaternary pump, a UV-visible detector and an autosampler, was used. The separation was carried out with an XTerra MS C18 column (150 mm  $\times$  4.6 mm i.d., 5  $\mu\text{m}$  particle size), using a guard column of similar characteristics (20 mm  $\times$  3.0 mm i.d., 5  $\mu\text{m}$  particle size) (Waters, MA, USA). The dead time (1.73 min) was measured as the first deviation of the baseline, and the dwell time (1.53 min) was detected by running a blank gradient where acetone increased from 0 to 1% in 20 min. Home built-in routines, written in MATLAB 6.5 (The Mathworks, Natick, MA, USA), were developed for data treatment. Other details are given elsewhere [10].

## 4. Results and discussion

### 4.1. Isocratic optimisation

An optimisation of the best isocratic conditions was performed first to separate the mixture of  $\beta$ -blockers. This offered a reference separation to evaluate the gradient results. An isocratic experimental design, consisting of six mobile phases containing 5, 10, 15, 20,

Table 1

Elementary and overall peak purities, and analysis times for the mixture of 16  $\beta$ -blockers in isocratic and gradient optimisations

Compound	Isocratic	Gradient <sup>a</sup>		
		$t_G$	$t_G, \varphi_0$	$t_G, \varphi_0, n$
Atenolol	0.999	0.776	0.998	0.998
Practolol	0.980	1.000	0.973	0.969
Sotalol	0.980	0.776	0.971	0.967
Nadolol	0.998	0.861	0.966	0.977
Carteolol	1.000	1.000	1.000	1.000
Pindolol	0.998	0.861	0.966	0.977
Metoprolol	1.000	0.998	0.997	0.998
Acebutolol	1.000	0.920	0.987	0.987
Esmolol	1.000	0.740	0.993	0.995
Celiprolol	0.990	0.739	0.993	0.995
Labetalol	0.997	1.000	1.000	1.000
Oxprenolol	1.000	1.000	1.000	1.000
Bisoprolol	0.990	1.000	1.000	1.000
Propranolol	0.997	0.970	0.989	0.993
Alprenolol	1.000	0.970	0.989	0.993
Timolol	1.000	0.922	0.990	0.989
Overall peak purity	0.932	0.194	0.827	0.847
Analysis time (min)	256	26.4	30.9	31.8

<sup>a</sup> The optimised factors are indicated.

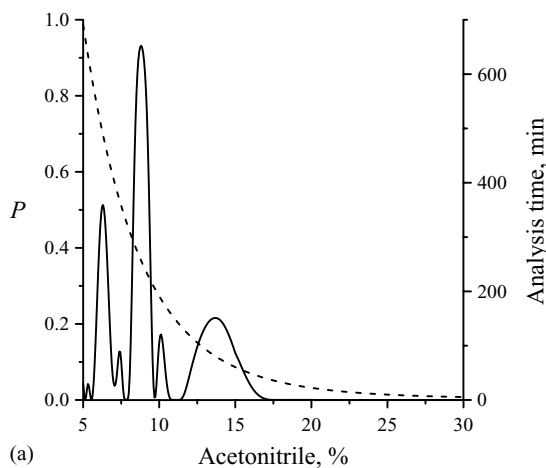
25 and 30% acetonitrile, was carried out. Only those mobile phases yielding retention times smaller than 60 min were considered.

The procedure followed to develop the isocratic optimisation can be found elsewhere [32]; it will be thus not detailed. Fig. 1a depicts the global resolution map, and Fig. 1b the best chromatogram found. Using the optimal mobile phase (8% acetonitrile,  $P = 0.93$ ), all solutes were almost baseline resolved (see also peak purities in Table 1). Unfortunately, the analysis time was unacceptable (>4 h), and expediting the analysis below 1 h without worsening the resolution to an intolerable level was not possible. The best resolution found with the analysis time restriction (15% acetonitrile) yields  $P < 0.1$ , which is too poor. Therefore, the use of gradient elution was mandatory in the considered example.

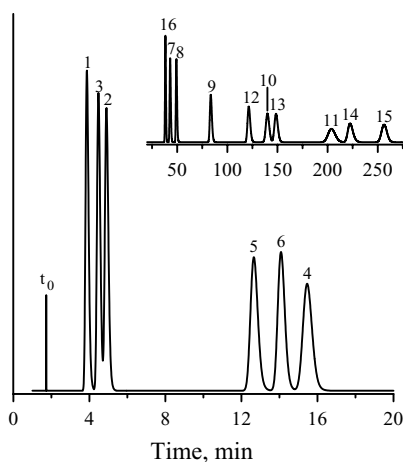
### 4.2. Gradient optimisation

#### 4.2.1. Modelling the peak shape in gradient conditions

Although in a first approximation, the shape parameters  $N$  and  $B/A$  can be considered constant at



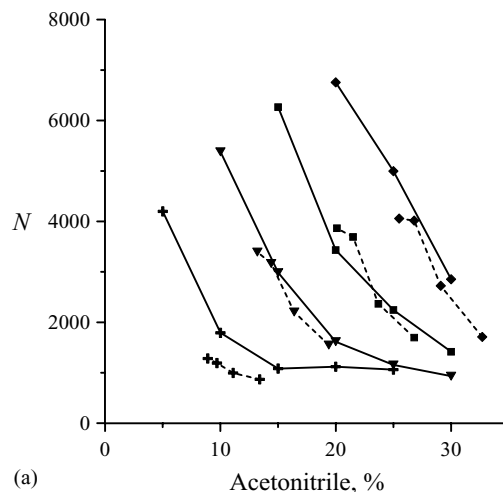
(a)



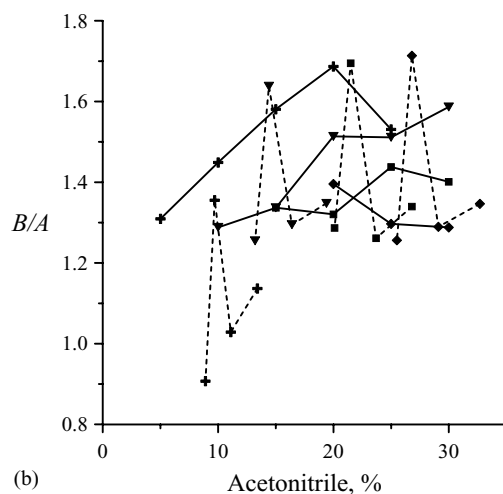
(b)

Fig. 1. (a) Map depicting the resolution measured as overall peak purity ( $P$ , solid line, left axis) and the analysis time (dashed line, right axis) achieved in the isocratic separation of a mixture of 16  $\beta$ -blockers, as a function of mobile phase composition, and (b) optimal chromatogram obtained at 8.0% acetonitrile–water ( $P = 0.93$ ). The analysis time was not considered as a factor in the optimisation. Compound identities: (1) atenolol, (2) practolol, (3) sotalol, (4) nadolol, (5) carteolol, (6) pindolol, (7) metoprolol, (8) acebutolol, (9) esmolol, (10) celiprolol, (11) labetalol, (12) oxprenolol, (13) bisoprolol, (14) propranolol, (15) alprenolol, and (16) timolol.

varying mobile phase composition, they actually depend on it. Fig. 2 illustrates such variations in both the isocratic-to-gradient and gradient-to-gradient predictions. In the latter case, the composition depicted in the X-axis corresponds to the instant gradient composition at the column outlet when the solute leaves the column.



(a)



(b)

Fig. 2. Variations in (a) efficiency and (b) asymmetry factor as a function of mobile phase composition in isocratic (solid lines) and gradient (dashed lines) experiments. In the latter case, the X-axis indicates the concentration of acetonitrile at which the solute leaves the column in the corresponding gradient run at the column outlet. Compound identities: sotalol (+), pindolol (▼), esmolol (■), and propranolol (◆).

As can be seen, smooth variations in both parameters are found for the isocratic-to-gradient case. This suggests the convenience of using local linear models to predict these variations. In contrast, gradient-to-gradient predictions of  $N$  and  $B/A$  are rather inaccurate, particularly for the latter, being practically unpredictable. In this case, the use of local linear models is very risky, especially when

extrapolations are required. This possibility cannot be discarded in these predictions, since the change in initial solvent composition may be interesting. A global trend (a straight line) was thus selected as an appropriate alternative to fit the  $N$  and  $B/A$  values for each solute.

#### 4.2.2. Optimisation of linear gradients from isocratic experimental data

The methodology outlined in Section 2 was next applied. The same data set previously introduced in the isocratic case was first considered to find the optimal gradient. The result obtained in this way can be considered as a reference for the comparison with the more practical gradient-to-gradient optimisation (see Section 4.2.4), since the accuracy in predictions of retention time is maximal (this will be discussed later).

A resolution matrix containing 21 levels in gradient slope ( $t_G$  from 20 to 50 min), and other 21 in initial solvent composition ( $\varphi_0$  from 5 to 15% acetonitrile) was computed. Fig. 3 shows the corresponding resolution map. This figure illustrates the suitability of the peak purity criterion as COF, to measure the resolution in gradient elution. As can be seen, the chromatographer appraisal strongly correlates with  $p$ -values. Drops of resolution are due to several peak reversals. The valley starting about  $t_G = 35$  min corresponds to the peak crossing of nadolol/pindolol, and that found between  $\varphi_0 = 10$  and 12% acetonitrile depicts the coelution of practolol/sotalol. Since the maximal  $P$ -value is  $<0.9$ , a slight coelution can be expected even at the optimal mobile phase (the critical peak pair is nadolol/pindolol, see Table 1).

Six chromatograms corresponding to representative points of the grid are also included in the figure. The resolution achieved with a gradient whose  $t_G$  and  $\varphi_0$ -values were 50 min and 6% acetonitrile, respectively, was insufficient (Fig. 3a,  $P = 0.59$ ): peak pairs 1/3 and 4/6 coelute. A better separation was found with a gradient starting at 9% acetonitrile using the same gradient time (Fig. 3b,  $P = 0.74$ ): peaks 1/3 are almost baseline resolved, but now peaks 2/3 coelute partially and the separation of peaks 4/6 is still not optimal. Fig. 3c ( $t_G = 50$  min,  $\varphi_0 = 13.5\%$ ), Fig. 3d ( $t_G = 35$  min,  $\varphi_0 = 5\%$ ), and Fig. 3e ( $t_G = 20$  min,  $\varphi_0 = 8.5\%$ ), represent three situations of poorer separation ( $P = 0.17$ , 0.006 and 0.10, respectively) due to the strong coelution of specific peak pairs.

The optimisation of the starting solvent concentration was essential. The optimal resolution obtained by fixing  $\varphi_0$  at 5% acetonitrile (univariate optimisation) was found at  $t_G = 26$  min. However,  $P$  was only 0.19 (Table 1). When both factors ( $t_G$  and  $\varphi_0$ ) were optimised, maximal resolution was found at 36.5 min and 8.5% acetonitrile ( $P = 0.83$ , see Fig. 3f). The resolution was notably enhanced, especially for the critical solutes. Only the peak purity of practolol decreased slightly. The chromatogram found was almost baseline resolved.

#### 4.2.3. Optimisation of curvilinear gradients from isocratic experimental data

Although the optimisation of  $t_G$  and  $\varphi_0$  yielded fairly acceptable results, the influence of the concavity/convexity of the gradient program as a third factor was also tested for an eventual enhancement of the separation. The procedure was similar to that followed in the previous section, but varying regularly this time three factors ( $t_G$ ,  $\varphi_0$  and  $n$ ). Thus, a  $21 \times 21 \times 21$  grid was computed, changing  $t_G$  and  $\varphi_0$  as before, and  $n$  from 0.1 to 2 (note that values of  $n = 0$  correspond to isocratic elution).

Due to the three factors involved, the results cannot be drawn as a single surface. For this reason, a simplified plot is shown instead, where each point represents the maximal resolution ( $P_{\max}$ ) found in a  $21 \times 21$  grid defined by keeping  $n$  constant and varying  $t_G$  and  $\varphi_0$  (i.e. a plot showing the maximal resolution as a function of the gradient curvature). The  $P_{\max}$  versus  $n$  dependence is plotted in Fig. 4a (full line, left axis), together with the analysis time of the corresponding optimal chromatogram (dashed line, right axis). Each  $t_G$  versus  $\varphi_0$  resolution surface presents several local maxima, which change in position and relative importance as  $n$  varies. Fig. 4b plots the optimal  $t_G$  and  $\varphi_0$  for each  $n$  value, which allows to follow the position of the main maximum. The overlaid vertical lines point out sudden changes in the relative importance of local maxima.

Fig. 5 shows the resolution surface corresponding to the optimal  $n$  value, where the full circle indicates the absolute best gradient condition ( $t_G = 50$  min,  $\varphi_0 = 8.5\%$  acetonitrile and  $n = 0.67$ ). The corresponding chromatogram is also given. For the  $\beta$ -blockers, the resolution achieved by including the gradient curvature as an additional factor ( $P = 0.85$ ) did not im-



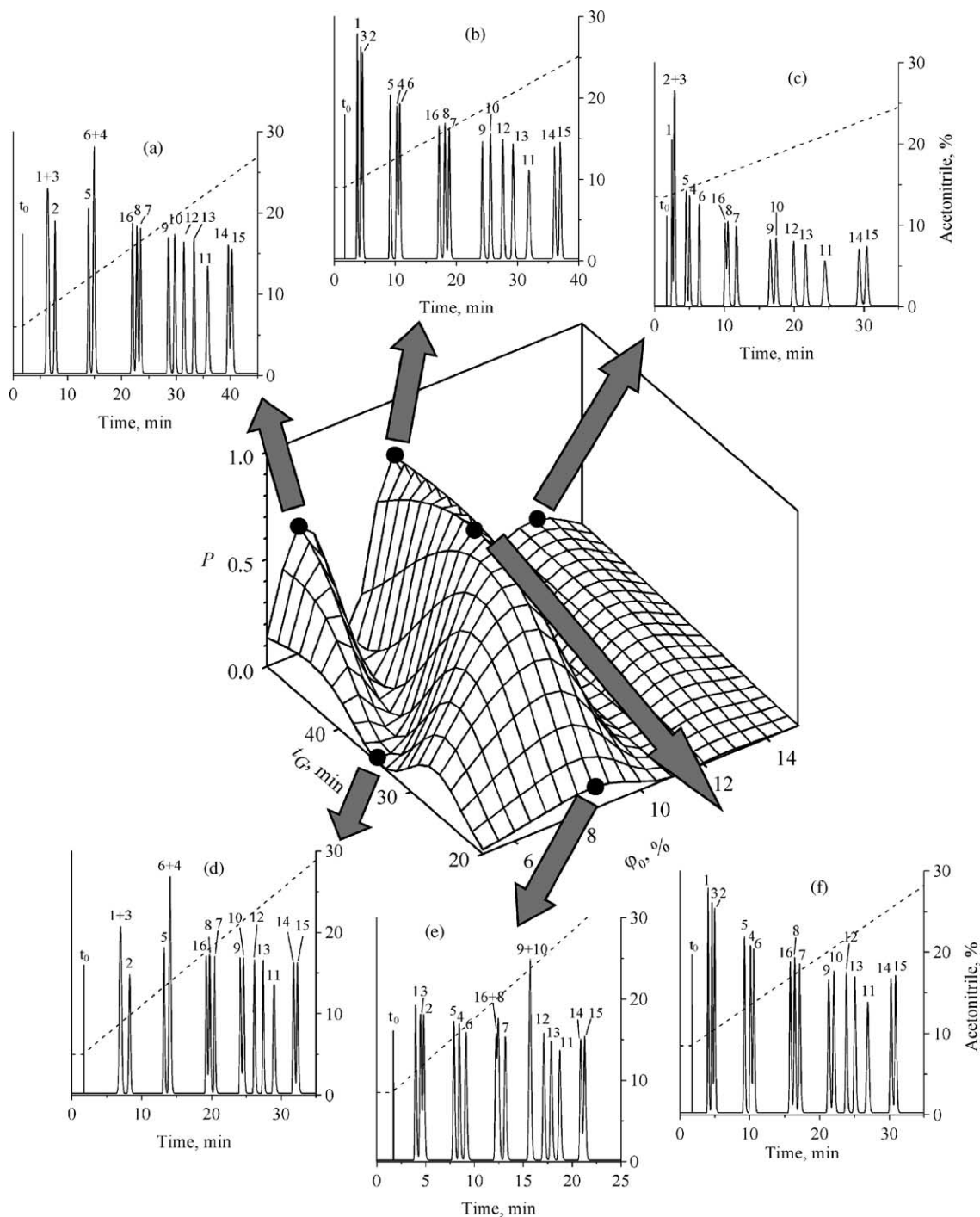


Fig. 3. Resolution surface of overall peak purity for the optimisation of gradient time ( $t_G$ ) and initial acetonitrile concentration ( $\phi_0$ ), in the separation of the 16  $\beta$ -blockers. Some representative chromatograms are given, corresponding to the gradients depicted by the full circles (see text for chromatographic conditions). Gradient programs are overlaid in each chromatogram (dashed lines, right axis).

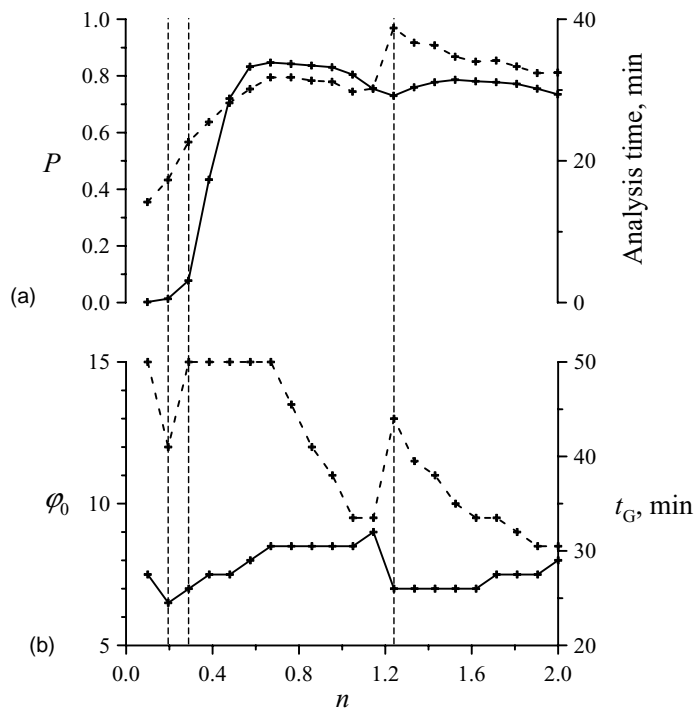


Fig. 4. (a) Maximal overall peak purity found in the optimisation of  $t_G$  and  $\varphi_0$  as a function of the gradient curvature,  $n$  (solid line, left axis), and analysis time at that optimal condition (dashed lines, right axis), and (b) optimal  $t_G$  (solid line) and  $\varphi_0$  (dashed line) for each  $n$  value.

prove significantly the separation achieved with the optimal linear gradient (see peak purities in Table 1). Note that  $n$  is clearly different from 1 and the optimal  $t_G$  is also different from the optimal linear gradient in Section 4.2.2. Nevertheless, the new gradient is close to the optimal gradient previously found: the convexity generated by  $n = 0.67$  is compensated by the increment in  $t_G$ . Accordingly, the chromatograms are virtually identical for both the linear and the curvilinear cases (compare Figs. 3f and 5). This explains why the resolution remains nearly constant between  $n = 0.6$  and 1.0 (Fig. 4): changes in  $n$  are compensated by reductions in  $t_G$ , which produces gradient programs close to the optimal linear gradient. Note that the optimal  $\varphi_0$  varies in a narrow range (6.5–9.0%), for different  $n$  values.

#### 4.2.4. Gradient optimisation from gradient experimental data

The performance of the optimisation when gradient experimental data are used in the modelling

step was also examined. A set of experiments where each  $\beta$ -blocker was eluted with four linear gradients, increasing the acetonitrile concentration from 5 to 30% in 20, 30, 40 and 50 min, was carried out. As before, peak widths and asymmetries together with retention times were considered in the optimisation. Note that this design does not include information about variations on  $\varphi_0$ . Since this descriptor was found to be essential in the success of the gradient optimisation, the possibility of expanding the predictions to gradients out of the domain covered by the gradient experimental design was first examined.

Gradients contain certain information that allow predictions at  $\varphi_0$ -values above those sampled by the training set. Indeed, predicting chromatograms for a starting mobile phase concentration not covered by the experimental design is not so risky as could be expected, since the actual variable being scanned through changing  $t_G$  and  $\varphi_0$  is the solvent concentration,  $\varphi$ . A study on the information that can be extracted from

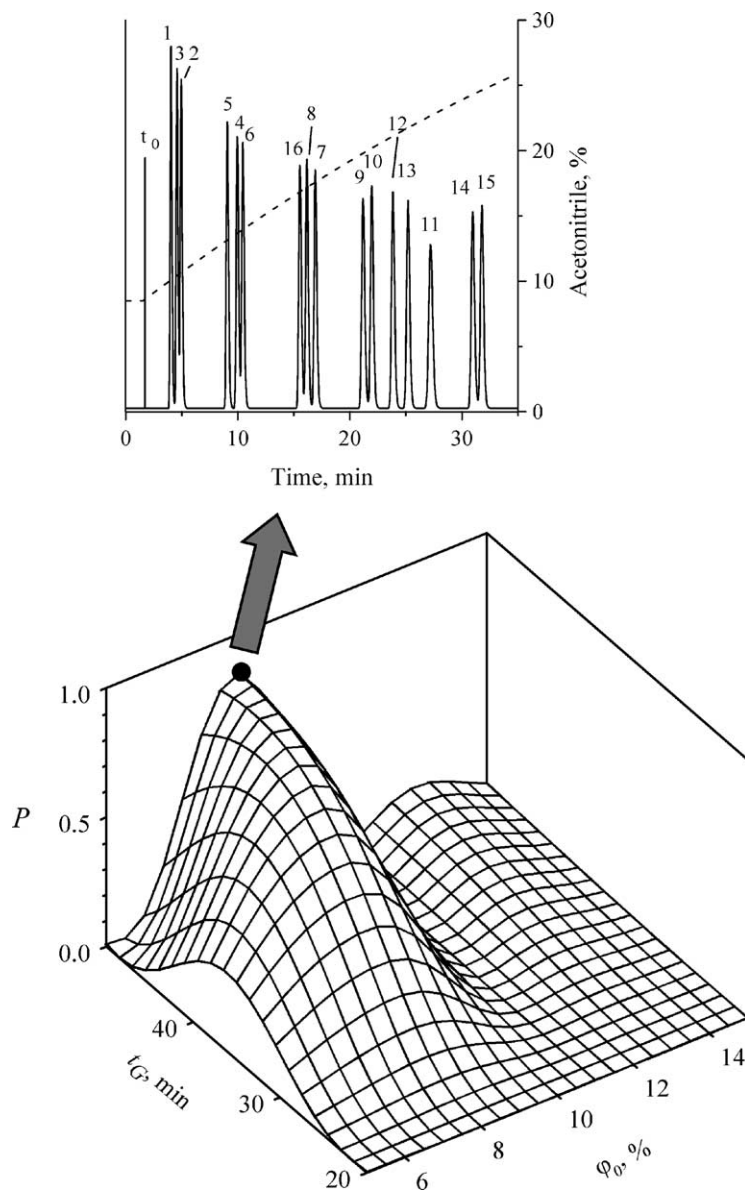


Fig. 5. Resolution surface of overall peak purity obtained for the optimal gradient curvature ( $n = 0.67$ ) and best chromatogram ( $t_G = 50$  min and  $\varphi_0 = 8.5\%$  acetonitrile). See Fig. 1 for compound identities.

the experimental design used in the modelling step was carried out according to Section 2.4. Values of  $\epsilon_{\text{norm}}$  for each solute were calculated according to two gradient experimental designs

- (i) The same experimental design used to model the retention (design A, including four gradients).
- (ii) A full experimental design of two factors at two levels ( $t_G = 20$  and  $50$  min, and  $\varphi_0 = 5$  and  $15\%$  acetonitrile) (design B).

The study of  $\epsilon_{\text{norm}}$  associated to both designs allowed a comparison between the information extracted from the experiments, and that required for

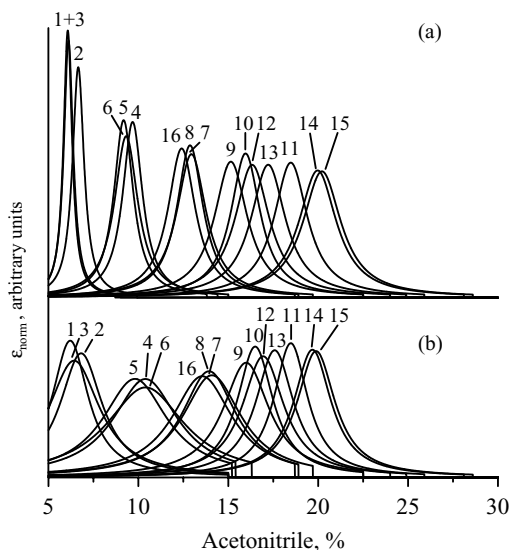


Fig. 6. Amount of information ( $\epsilon_{\text{norm}}$ ) as a function of acetonitrile concentration for the 16  $\beta$ -blockers, according to two experimental designs: (a) four gradients changing the mobile phase composition from 5 to 30% acetonitrile in 20, 30, 40 and 50 min, and (b) two gradients changing from 5 to 30% acetonitrile in 20 and 50 min, and other two from 15 to 30% acetonitrile in 20 and 50 min. See Fig. 1 for compound identities.

the predictions. Note that no isocratic data were used in this evaluation: only gradient experiments fitted with Eq. (1) were considered. Fig. 6a and b show the amount of information as a function of mobile phase composition associated to designs A and B, for the set of 16  $\beta$ -blockers. Each compound gave a smooth variation of  $\epsilon_{\text{norm}}$ , that suddenly dropped to zero at a critical composition: the  $\varphi$ -value for the fastest gradient program at which the solute leaves the column. Solvent concentrations greater than these critical values did not affect the solutes in any of the tested gradients (see Section 2.4, step (v)).

The differences between  $\epsilon_{\text{norm}}$ -values obtained with the two designs depend on the retention behaviour of each solute. Design A (Fig. 6a) provides, for the less retained compounds (solutes 1–8 and 16), maximal information in narrow ranges of acetonitrile concentration, with  $\epsilon_{\text{norm}}$ -profiles sharper than those obtained for design B. This means that the latter design is more informative for these solutes. As a result, predictions of retention inside the experimental domain covered by design B from the data in design A, will require a

certain level of extrapolation. In contrast, the profiles of the slowest solutes (solutes 9–15) were practically identical using both designs, which indicates that they are similarly informative. For these solutes, the retention for gradients using  $\varphi_0$ -values out of the domain covered by design A can be predicted without requiring an extrapolation.

An analysis of the process happening inside the column reveals why both designs yield so different information. During a linear gradient, solutes undergo an exponential increment in migration speed, which is reflected in the exponential  $k$  versus  $\varphi$  dependence in Eqs. (1)–(3). As a consequence, only those mobile phase compositions where the migration speed is significant contribute to the overall retention behaviour. For the slowest solutes, the migration is negligible at the beginning of the gradient, independently of the starting concentration tested (5% or 15% acetonitrile), which makes designs A and B to perform similarly. This does not happen for the fastest solutes, since in the

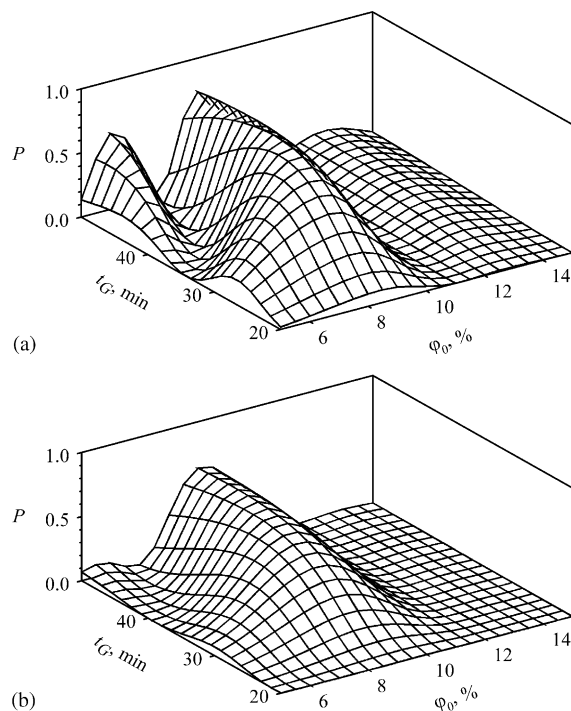


Fig. 7. Resolution maps of overall peak purity for the gradient optimisation in the separation of 16  $\beta$ -blockers when the data are collected from: (a) isocratic, and (b) gradient experiments. Eqs. (2) and (3) were used in (a) and (b), respectively.

5–15% acetonitrile range the migration rate is appreciable even at the beginning of the gradient, which is translated in the different performance of both designs. Since a certain extrapolation capability is needed to model the retention using design A to predict gradients out of its  $\varphi_0$  domain, a retention model with a good extrapolation performance (Eq. (3)) [10] was used.

The optimisation of the gradient program was faced using the same methodology described in Section 4.2.2 for isocratic elution. The resolution maps obtained from isocratic and gradient data are presented in Fig. 7a and b, respectively. Although both figures look rather similar, some differences are perceptible in the region of low  $\varphi_0$  and high  $t_G$  values. This region is especially sensitive to the behaviour of the critical peak pairs 1/3 and 4/6, and minor differences attributable to gradient time predictions (due to the particular behaviour of each model and the different experimental data) can produce drastic changes in resolution. The optimal chromatograms with both approaches are however almost identical.

## 5. Conclusions

The performance of isocratic and gradient separations was compared in an example involving 16  $\beta$ -blockers. The analysis time found for the optimal composition in isocratic elution—almost 4 h—was unacceptable. Unlike these results, gradient elution gave rise to a very competitive solution, being able to resolve the mixture almost up to the baseline in less than 35 min. Curvilinear gradients were not required for this sample.

The prediction of retention under gradient elution was studied using both isocratic and gradient experiments as training data. The first elution mode provides richer information about the behaviour of the chromatographic system, but the experimental data are more laborious to obtain and not so useful in practice. Meanwhile, gradient training data are less informative and may require a detailed study on the retention information gathered by the experimental design.

Gradient-to-gradient optimisation demanded in the example shown an increment of the initial solvent compositions assayed,  $\varphi_0$ . Analysis of errors is demonstrated to be a worthy tool to assess the extrapolation level required in such situations. This analysis

allows relating rigorously the amount of information gathered from the experiments to particular values of solvent composition in the mobile phase, which is the true subjacent factor being modelled. Our study indicated that the extrapolation extent is often not so large as the change in  $\varphi_0$  apparently suggests. In the considered example, only the prediction of the fastest solutes is done throughout an extrapolation when  $\varphi_0$  was increased. In order to avoid inaccurate predictions for these solutes, an equation with a contrasted good performance in extrapolations, such as Eq. (3), is recommended for the prediction of gradient chromatograms from gradient training sets.

Peak purity is shown as a suitable criterion in gradient optimisation, provided that peak width and, in a lesser extent, the asymmetry, are conveniently modelled. Variations in efficiency and asymmetry factor in gradient-to-gradient predictions are more difficult to model than in the isocratic-to-gradient case. This makes the use of global models more appropriate in the former case, while local models are suitable in the second case.

## Acknowledgements

This work was supported by Project BQU2001–3047 (Ministerio de Ciencia y Tecnología of Spain) and Project CTIDIB/2002/226 (Generalitat Valenciana). JR TL and GVT thank the MCYT for a Ramón y Cajal position, and the Generalitat Valenciana for an FPI grant, respectively.

## References

- [1] J.W. Dolan, D.C. Lommen, L.R. Snyder, *J. Chromatogr.* 485 (1989) 91.
- [2] H.J. Rieger, I. Molnar, *J. Chromatogr. A* 948 (2002) 43.
- [3] R. Cela, M. Lores, *Comput. Chem.* 20 (1996) 175.
- [4] S. Heinisch, E. Lesellier, C. Podevin, J.L. Rocca, A. Tchaplá, *Chromatographia* 44 (1997) 529.
- [5] W.D. Beinert, R. Jack, V. Eckert, S. Galushko, V. Tanchuck, I. Shishkina, *Int. Lab.* 31 (2001) 16.
- [6] N. Lundell, *J. Chromatogr.* 639 (1993) 97.
- [7] J.C. Ford, J. Ko, *J. Chromatogr. A* 727 (1996) 1.
- [8] M.A. Quarry, R.L. Grob, L.R. Snyder, *Anal. Chem.* 58 (1986) 907.
- [9] B.F.D. Ghrist, B.S. Cooperman, L.R. Snyder, *J. Chromatogr.* 459 (1988) 1.

- [10] G. Vivó-Truyols, J.R. Torres-Lapasió, M.C. García-Alvarez-Coque, *J. Chromatogr. A* 1018 (2003) 169.
- [11] P.J. Schoenmakers, H.A.H. Billiet, L. de Galan, *J. Chromatogr.* 185 (1979) 179.
- [12] M. Rosés, E. Bosch, *Anal. Chim. Acta* 274 (1993) 147.
- [13] J.R. Torres-Lapasió, M.C. García-Alvarez-Coque, M. Rosés, E. Bosch, *J. Chromatogr. A* 955 (2002) 19.
- [14] P. Jandera, *J. Chromatogr. A* 845 (1999) 133.
- [15] L.R. Snyder, J.L. Glajch, J.J. Kirkland, *Practical HPLC Method Development*, second edition, Wiley/Interscience, New York, 1997 (Chapter 8).
- [16] P. Chaminade, A. Baillet, D. Ferrier, *J. Chromatogr. A* 672 (1994) 67.
- [17] S. Carda-Broch, J.R. Torres-Lapasió, M.C. García-Alvarez-Coque, *Anal. Chim. Acta* 396 (1999) 61.
- [18] S.J. López-Grío, G. Vivó-Truyols, J.R. Torres-Lapasió, M.C. García-Alvarez-Coque, *Anal. Chim. Acta* 433 (2001) 187.
- [19] J.M. Cruickshank, *Beta-Blockers in Clinical Practice*, Churchill-Livingstone, New York, 1994.
- [20] L.R. Snyder, in: Cs. Horváth (Ed.), *High Performance Liquid Chromatography. Advances and Perspectives*, Academic Press, London, 1983, p. 207.
- [21] L.R. Snyder, J.W. Dolan, *Adv. Chromatogr.* 38 (1998) 115.
- [22] W.H. Press, S.A. Teukolsky, W.T. Vetterling, B.P. Flannery, *Numerical Recipes in C*, second edition, Cambridge University Press, Cambridge, 1992.
- [23] J.P. Foley, J.G. Dorsey, *Anal. Chem.* 55 (1983) 730.
- [24] J.R. Torres-Lapasió, J.J. Baeza-Baeza, M.C. García-Alvarez-Coque, *Anal. Chem.* 69 (1997) 3822.
- [25] P. Jandera, *J. Chromatogr.* 485 (1989) 113.
- [26] G. Vivó-Truyols, J.R. Torres-Lapasió, M.C. García-Alvarez-Coque, *J. Chromatogr. A* 876 (2000) 17.
- [27] V. Di Marco, G.G. Bombi, *J. Chromatogr. A* 931 (2001) 1.
- [28] J.R. Torres-Lapasió, D.L. Massart, J.J. Baeza-Baeza, M.C. García-Alvarez-Coque, *Chromatographia* 51 (2000) 101.
- [29] G. Vivó-Truyols, J.R. Torres-Lapasió, M.C. García-Alvarez-Coque, *J. Chromatogr. A* 991 (2003) 47.
- [30] S. López-Grío, J.R. Torres-Lapasió, J.J. Baeza-Baeza, M.C. García-Alvarez-Coque, *Anal. Chim. Acta* 418 (2000) 153.
- [31] G. Vivó-Truyols, J.R. Torres-Lapasió, M.C. García-Alvarez-Coque, *Chromatographia* 56 (2002) 699.
- [32] J.R. Torres-Lapasió, M. Rosés, E. Bosch, M.C. García-Alvarez-Coque, *J. Chromatogr. A* 886 (2000) 31.